

Ground-state properties of generalized Heisenberg chains with composite spin

J. Sólyom*

Institut Laue-Langevin, 156X, F-38042 Grenoble, France

J. Timonen

Department of Physics, University of Jyväskylä, SF-40100 Jyväskylä, Finland

(Received 1 April 1988)

We consider in detail the ground-state properties of recently introduced generalized Heisenberg models which can have several spin operators at each site and which interpolate smoothly between Heisenberg chains of different spin lengths. We show that the mappings to field-theoretical models used to describe the critical properties of the Heisenberg model remain valid in the composite-spin model. In models which interpolate between the spin- $\frac{1}{2}$ and the spin-1 behavior, these mappings predict an extended singlet phase around the isotropic antiferromagnetic point whenever the models move away from the spin- $\frac{1}{2}$ point. Numerical calculations on finite chains seem to confirm the existence of this singlet phase. The phase boundaries are, however, found to be independent of the interpolation parameter, and thus in disagreement with the predictions of the continuum theory, indicating its limitation.

I. INTRODUCTION

In a recent paper¹ we have introduced composite spin models with a generalized Heisenberg-like interaction. It has been shown that with the appropriate choice of the coupling constants, the low-lying levels of the composite-spin models will coincide with those of the usual Heisenberg chain with arbitrary spin. The extra states introduced by the extra degrees of freedom of the composite spin do not mix, in special cases, to the other levels and lie higher in energy. It was also shown that this makes it possible to connect continuously, by changing a single parameter, Heisenberg models with different spins.

This possibility is of special interest in light of a surprising prediction by Haldane,² according to which half-integer and integer spin Heisenberg models behave drastically differently when the coupling is antiferromagnetic. Near the isotropic antiferromagnetic point for integer spins the ground state is a nondegenerate singlet state, separated from the first excited state by a finite gap. This so-called Heisenberg-singlet phase appears in a relatively narrow region between the antiferromagnetic, the massless planar, and the usual massive singlet phases. For half-integer spins, however, this Heisenberg-singlet phase cannot exist, the antiferromagnetic and planar phases meet at the isotropic antiferromagnetic point.

A lot of numerical work has been devoted to study this problem.³⁻¹¹ The numerical results for the $S=1$ model indicate quite strongly the existence of a finite gap at the isotropic point, the strongest evidence being the Monte Carlo calculation⁷ for rather long chains (up to 32 sites), although other calculations⁸ on chains with 40 sites gave contradictory results. Due to the spin quantization the calculations using the original Heisenberg Hamiltonian have to be done separately for integer and half-integer

spins. Having at our disposal the composite-spin model where integer and half-integer spin situations can be considered in the same framework, it seemed to us that it could shed some light on the mechanism of this mass generation. In this spirit we have undertaken analytical and numerical studies of the composite spin model taking two or more spins at a site and using different choices of the coupling constants.

The model and its relationship to the usual Heisenberg chain with arbitrary spin is presented in Sec. II. When the spin is composed of $S = \frac{1}{2}$ operators, various transformations can be used to study the properties of the model in the continuum limit, as discussed in Sec. III. In Sec. IV we show first the numerical results for the case when the composite spin model interpolates between $S = \frac{1}{2}$ and $S = \frac{3}{2}$ behavior. The results obtained here serve as a guide for how reliable the numerical calculations on the available chain lengths can be. The problem of the Heisenberg-singlet phase is treated in Sec. V. Finally a discussion of the analytic and numerical results is given in Sec. VI.

II. DEFINITION OF THE COMPOSITE-SPIN MODELS

A composite-spin model was recently proposed¹ by us where at each lattice site i there are two or more spin operators $\sigma_{i\alpha}$ ($\alpha = 1, 2, \dots$) with arbitrary spin lengths. We assume that the interaction is of short range in space, and consider on-site and nearest-neighbor interactions only. On the other hand a spin species α interacts with all spin species on the same site or on nearest-neighbor sites. The Hamiltonian can be decomposed into a sum

$$H = \sum_{\alpha, \beta} H_{\alpha\beta}, \quad (2.1)$$

where $H_{\alpha\beta}$ describes the interaction between spin species

α and β .

Furthermore, it will be assumed that each of the terms $H_{\alpha\beta}$ is of the same form. It contains a usual Heisenberg exchange with a possibility for anisotropy in the longitudinal terms only and an on-site coupling between the z components of the spins

$$H_{\alpha\beta} = -\frac{1}{2}J_{xy}^{\alpha\beta} \sum_{i,j} (\sigma_{i\alpha}^+ \sigma_{j\beta}^- + \sigma_{i\alpha}^- \sigma_{j\beta}^+) - J_z^{\alpha\beta} \sum_{i,j} \sigma_{i\alpha}^z \sigma_{j\beta}^z + D^{\alpha\beta} \sum_i \sigma_{i\alpha}^z \sigma_{i\beta}^z, \quad (2.2)$$

where the xy term is written in terms of the raising and lowering operators.

In general, if there are p different species of spins, there are $3p^2$ different coupling parameters in the Hamiltonian. One of the parameters can be chosen as setting the energy scale so the dimension of the phase space is $3p^2 - 1$. This is too large for any practical calculation even for two different spin species and it is useful to consider two-dimensional sections of the phase space by choosing simple parametrizations.

Let us consider first models where $D^{\alpha\beta} = 0$. A particularly simple parametrization is

$$J_k^{\alpha\beta} = \begin{cases} J_k, & \text{for } \alpha = \beta \\ \lambda J_k, & \text{for } \alpha \neq \beta \end{cases} \quad (2.3)$$

which results in a two-dimensional phase space for all p . Here $k = xy$ or z . We have done detailed calculations only in the cases $p = 2, 3$ and $\sigma_\alpha = \frac{1}{2}, 1$, but it is easy to generalize some of the results to arbitrary values of these parameters.

It is clear that at $\lambda = 0$, the model reduces to that of p decoupled spin chains with their individual spin lengths. For finite λ , when the different spin species are coupled, in general little is known about the behavior of the model. At $\lambda = 1$, however, the ground state of the model given by Eqs. (2.1)–(2.3) is identical to that of a Heisenberg model with spin $S_p = \sum_{\alpha=i}^p \sigma_\alpha$. Although this statement is not trivial, it is not surprising either, as will be shown below.

The Hilbert space of the problem is a direct product of the spin states of the different spin species. Using the rules of addition of the angular momentum, this Hilbert space can be sectorized according to the length of the total spin on a site, $S_p, S_p - 1, S_p - 2, \dots$. Using as basis states the eigenstates of the z component of the spin from each sector, the Hamiltonian will mix states from different sectors. A particular simplification arises at $\lambda = 1$. Namely, at this point the Hamiltonian will behave as the usual Heisenberg exchange Hamiltonian. The S^z projections of neighboring spin states can be changed, one is lowered, the other is raised, but the spin length is not modified. The spin length on any site is conserved. The ground-state energy is in the sector where at each site the spin length is the largest, i.e., the ground state is identical to that of a Heisenberg model with spin S_p . The low-lying states are also identical. The first extra states compared to the spin- S_p Heisenberg model are those where at one site a spin S_p is replaced by a spin of length $S_p - 1$. At $\lambda = 1$ this spin can be considered as an immo-

bile magnetic defect in the chain. Because of the shorter spin length, this state is separated from the ground state by a finite energy. In the ‘‘planar’’ region, $-J_{xy} < J_z < J_{xy}$ this energy difference is $\Delta E = 2S_p J_{xy}$ in the limit $N \rightarrow \infty$. In the ferromagnetic region $J_z > J_{xy}$ this energy difference is $\Delta E = 2S_p J_z$. Taking the absolute value of J_z this is also true on the antiferromagnetic side, away from the isotropic point, where the Néel state is a good approximation.

Since, as mentioned above, at $\lambda = 0$ the properties of the model are those of independent chains with spin length σ_α , while at $\lambda = 1$ the behavior of a magnetic system with spin $S_p = \sum_\alpha \sigma_\alpha$ is recovered, in a model where λ varies from zero to 1, the behavior of the model should vary from that corresponding to a spin- σ_α chain to that corresponding to a spin- S_p chain. How smooth that variation is and what we can learn from it will be the subject of the further sections.

An interesting and potentially useful feature of parametrization (2.3) is the behavior under canonical transformation of spin variables. When $p = 2$ and the two spin species have the same length, interchanging the two spin operators on every other site gives the same problem with modified parameters, J_k in (2.3) replaced by λJ_k and λJ_k by J_k . Consequently, all the energy levels satisfy a simple self-duality relation

$$E(\lambda) = \lambda E(1/\lambda). \quad (2.4)$$

This duality relation is helpful in studying the scaling behavior of energy levels since it holds for finite chains, too. The duality relation (2.4) relates the weak-coupling situation $0 \leq \lambda \leq 1$ to the strong coupling case $1 \leq \lambda < \infty$. The case $\lambda = 0$, where the coupling between different spin species vanishes, is related by duality to $\lambda = \infty$ where the coupling between identical spin species can be neglected. However, the type of the ground state is the same in the two cases. For $\lambda < 0$, the model would include both ferromagnetic and antiferromagnetic couplings and by varying λ the character of the ground state would change accordingly. It is clear that the duality relations are valid for $\lambda > 0$ only.

It is desirable to have other routes in the phase space for interpolating between the $\lambda = 0$ and $\lambda = 1$ systems, and therefore we look for other parametrization that satisfy the duality relationship. Another parametrization with such features is one where one spin species ($\alpha = 1$) plays a distinct role. The couplings J_k^{11} between the spins of this species are denoted by J_k ($k = xy, z$), while the couplings $J_k^{1\beta}$ of these spins to the other spin species ($\beta \neq 1$) and the couplings $J_k^{\alpha\beta}$ between the other spin species ($\alpha, \beta \neq 1$) are chosen as

$$J_k^{1\beta} = J_k^{\beta 1} = \sqrt{\lambda} J_k^{11} = \sqrt{\lambda} J_k, \quad \beta \neq 1 \quad (2.5a)$$

$$J_k^{\alpha,\beta} = \lambda J_k, \quad \alpha, \beta \neq 1.$$

This parametrization defines again a two-dimensional surface in the phase space. The system is now reduced at $\lambda = 0$ to a single Heisenberg chain with $S = \sigma_1$ and a collection of independent, free spins. At $\lambda = 1$ its behavior is exactly the same as described above.

For $p=2$ and identical spin length S , parametrization (2.5a) leads, by a trivial interchange of spins at each site, to a self-duality relation for the energy levels E_a of the Hamiltonian.

For any $p > 2$ relation (2.4) does not hold, but parametrization (2.5a) is dual to

$$\begin{aligned} J_k^{11} &= \lambda J_k, \\ J_k^{1\beta} &= J_k^{\beta 1} = \sqrt{\lambda} J_k, \quad \beta \neq 1 \\ J_k^{\alpha\beta} &= J_k, \quad \alpha, \beta \neq 1 \end{aligned} \quad (2.5b)$$

in the sense that the energy levels E_b resulting from this parametrization are related to E_a by

$$E_a(\lambda) = \lambda E_b(1/\lambda). \quad (2.6)$$

When $p > 2$, further interesting parametrizations can be found that satisfy the duality relationship. One such parametrization is the "helical" parametrization. When all the spin lengths are identical, we take the following choice

$$\begin{aligned} J_k^{\alpha,\alpha} &= J_k, \\ J_k^{\alpha,\alpha+1} &= \lambda^{1/(p-1)} J_k, \\ J_k^{\alpha,\alpha+2} &= \lambda^{2/(p-1)} J_k, \\ &\vdots \\ J_k^{\alpha,\alpha+p-1} &= \lambda J_k, \end{aligned} \quad (2.7)$$

where the index of the species should be taken mod p . Due to the helical symmetry of this parametrization the energy levels satisfy (2.4), if the number of sites on the chain is a multiple of p .

All the parametrizations defined so far conserve the anisotropy, the couplings between the xy and z components have the same λ factors. The spin- $\frac{1}{2}$ model at $\lambda=0$ and the spin-1 model at $\lambda=1$ have the same anisotropy J_z/J_{xy} . Yet another interesting parametrization for $p=2$ can be chosen in the following way:

$$\begin{aligned} J_{xy}^{\alpha\alpha} &= J_{xy}^{\beta\beta} = J_{xy}, \quad J_{xy}^{\alpha\beta} = J_{xy}^{\beta\alpha} = \lambda J_{xy}, \\ J_z^{\alpha\alpha} &= J_z^{\beta\beta} = \lambda^q J_z, \quad J_z^{\alpha\beta} = J_z^{\beta\alpha} = \lambda^{1-q} J_z, \end{aligned} \quad (2.8)$$

where q is an arbitrary exponent.

At $\lambda=0$ this model reduces to two decoupled spin- $\frac{1}{2}$ XY models, while at $\lambda=1$ an anisotropic spin-1 Heisenberg model is recovered. Moreover, it is easily seen that the model satisfies the duality relationship.

When the on-site terms with $D^{\alpha\beta}$ in (2.2) are included, we will use two parametrizations. One possibility will be to take

$$D^{\alpha\beta} = \begin{cases} D & \text{if } \alpha = \beta \\ \lambda D & \text{if } \alpha \neq \beta. \end{cases} \quad (2.9)$$

The term $D^{\alpha\alpha}$ will give an uninteresting constant if the σ^α operators are spin- $\frac{1}{2}$ operators and at $\lambda=0$ the decoupled spin problems are recovered. At $\lambda=1$ the term with D will act as a single-ion anisotropy

$$H_D = D \sum_i (S_i^z)^2, \quad (2.10)$$

where

$$S_i^z = \sum_{\alpha=1}^p \sigma_{i\alpha}^z. \quad (2.11)$$

The single-ion anisotropy parameter D gives a new dimension in phase space and allows us to study the appearance of the singlet phase for large D as λ varies from $\lambda=0$ to $\lambda=1$.

This model does not satisfy self-duality. This property can be restored with the choice

$$D^{\alpha\alpha} = D^{\alpha\beta} = \sqrt{\lambda} D. \quad (2.12)$$

III. INFINITE CHAIN RESULTS

In this section we give a short account of the results which have been obtained for infinite spin chains, either discrete or in the continuum limit. We then extend the continuum limit results to cover the composite spin model which is of main concern here.

Let us first recall that the only soluble Heisenberg chain of the form considered here is that with spin $S = \frac{1}{2}$. In this case the ground state and the excitation spectrum of Hamiltonian (2.2) for a single spin species [the $(\sigma^z)^2$ term gives now a constant] can be solved exactly by using the Bethe ansatz¹² or the quantum inverse method.¹³ For $J_z < -J_{xy} < 0$ the ground state of the model is an antiferromagnetically ordered Néel-like state with a finite gap in the excitation spectrum. For $-J_{xy} < J_z < J_{xy}$ the ground state has a planar symmetry and there is a gapless excitation spectrum, and for $J_z > J_{xy} > 0$ the ground state has a ferromagnetic order and the excitation spectrum has a gap.

For general S the usual Heisenberg Hamiltonian is rewritten in the form

$$H = J \sum_j [\mathbf{S}_j \cdot \mathbf{S}_{j+1} + \gamma S_j^z S_{j+1}^z + \mu (S_j^z)^2], \quad (3.1)$$

thus including both longitudinal exchange (γ) and single-site (μ) anisotropy, and we will look for a continuum limit representation of it. As pointed out by Haldane,² one possibility is to use the classical angle representation for the spins,

$$\mathbf{S}_j = (-1)^j S (\sin\theta_j \cos\phi_j, \sin\theta_j \sin\phi_j, \cos\theta_j), \quad (3.2)$$

where a nearly antiferromagnetic alignment of spins is assumed.

In the harmonic approximation the magnon spectrum of the resulting Hamiltonian becomes soft both at $k=0$ and $k=\pi$ when $\gamma-\mu$ tends to zero. To include both of these soft modes continuum-limit variables $\theta(x)$, $\alpha(x)$, $\phi(x)$, and $\beta(x)$ are defined by

$$\begin{aligned} \theta_j &= \theta(x) + a(-1)^j \alpha(x), \\ \phi_j &= \phi(x) + a(-1)^j \beta(x), \end{aligned} \quad (3.3)$$

where $x \equiv ja$, and θ , α , ϕ , and β are assumed to be slowly varying fields. A consistent continuum limit can now be defined by expanding to second order in a and then letting $S \rightarrow \infty$ and $a \rightarrow 0$, and assuming that the sound velocity $c = 2aS$ and the magnon mass gap

$$\omega_0^2 \equiv 8S^2(\gamma - \mu) \tag{3.4}$$

remain finite. The spin length appears in the dimensionless coupling constant g as

$$g \equiv \frac{2}{S} . \tag{3.5}$$

Defining momentum variables

$$\begin{aligned} L(x) &\equiv -\frac{2}{g}\alpha \sin\theta , \\ \Pi(x) &\equiv \frac{2}{g}\beta \sin\theta , \end{aligned} \tag{3.6}$$

we can finally express the Hamiltonian (3.1) in the form

$$H = H_0 + H_1 , \tag{3.7a}$$

$$H_0 = \frac{cJ}{2} \int dx \left\{ g \left[\Pi^2 + \left(\frac{L}{\sin\theta} \right)^2 \right] + \frac{1}{g} \left[(\nabla\theta)^2 + \left(\frac{\omega_0^2}{c^2} + (\nabla\phi)^2 \right) \sin^2\theta \right] \right\} , \tag{3.7b}$$

$$H_1 = \frac{cJ}{2} \int dx \left\{ g \left[\left(\frac{\gamma + \mu}{2} \right) L^2 + \left(\frac{g\omega_0}{8} \right)^2 L^2 \cot^2\theta \right] + \frac{1}{g} \gamma (\nabla \cos\theta)^2 \right\} , \tag{3.7c}$$

where we have dropped an immaterial constant.

The first term H_0 can be identified with the Hamiltonian of the O(3) nonlinear sigma model. The variables in H_0 form canonically conjugate pairs of scalar fields which obey the Poisson bracket algebra $\{\phi(x), L(x')\} = \{\theta(x), \Pi(x')\} = \delta(x - x')$. If we define the vector field

$$\mathbf{n}_H = (\sin\theta \cos\phi, \sin\theta \sin\phi, \cos\theta) \tag{3.8}$$

so that $\mathbf{n}_H^2 = 1$, there will be a related momentum field \mathbf{p}_H such that $\{n_H^i(x), p_H^j(x')\} = \epsilon^{ijk} n_H^k(x) \delta(x - x')$ and $\mathbf{p}_H^2 = \Pi^2 + (L/\sin\theta)^2$. With these variables the Hamiltonian H_0 takes in fact the usual nonlinear σ -model form

$$H_0 = \frac{cJ}{2} \int dx \left\{ g \mathbf{p}_H^2 + \frac{1}{g} \left[(\nabla \mathbf{n}_H)^2 - \left(\frac{\omega_0}{c} \right)^2 (n_H^z)^2 \right] \right\} \tag{3.9}$$

with an extra anisotropic term proportional to ω_0^2 .

H_1 can be neglected in the leading order in the coupling constant, since all the terms in H_1 are of the order $g^2 \rightarrow 0$ compared with the terms in H_0 .

For $\omega_0 > 0$ the Hamiltonian (3.7) has two kinds of excitations, the ordinary spin-1 Néel magnons with a gap of ω_0 and nonlinear kink-like excitations which have semi-classically quantized gaps $M_n = \omega_0(n^2 + S^2)^{1/2}$. The parameter n is the eigenvalue of S^z for kinks and it is an integer for the integer spin models and a half-integer for the half-integer spin models. Haldane then argues that this picture is correct for finite anisotropies only. When $\omega_0 \rightarrow 0$, the nonlinear vacuum fluctuations will renormalize g to strong coupling. This leads to a “dynamic generation” of a gap ϵ_0 ,

$$\epsilon_0 \sim cJg e^{-2\pi g^{-1}} , \tag{3.10}$$

in the magnon spectrum. Consequently, the collective magnon excitations remain massive when the isotropic antiferromagnetic point $\omega_0 = 0$ is approached while the lowest kink mass $M_0 = 2\omega_0 g^{-1}$ is renormalized such that

it becomes soft at a finite anisotropy. The related transition is from a doubly degenerate antiferromagnetic ground state to nondegenerate singlet ground state and is thus of the Onsager type.

In the half-integer spin case the coupling constant is also renormalized to a large value, but there is no “dynamic mass generation,” and both the magnons and the kinks, $M_n \geq M_{\pm 1/2} = \omega_0(\frac{1}{4} + g^{-2})^{1/2} \sim \omega_0/2$, become soft only at the isotropic point $\omega_0 = 0$. The related transition is thus to an infinitely degenerate gapless state and is of the Kosterlitz-Thouless type. Notice that also in the half-integer spin case the lowest excitations close to the isotropic point are of the order destroying kink type, namely the lowest $M_{\pm 1/2}$ kinks. In the integrable $S = \frac{1}{2}$ model there are no spin-1 magnons and spin- $\frac{1}{2}$ kinks are the only excitations.

Another variant¹⁴ of the continuum limit of Hamiltonian (3.1) is provided by transformation

$$\begin{aligned} \mathbf{n}_{2j} &= \frac{1}{2S} (\mathbf{S}_{2j+1} - \mathbf{S}_{2j}) , \\ \mathbf{p}_{2j} &= \frac{1}{2a} (\mathbf{S}_{2j+1} + \mathbf{S}_{2j}) , \end{aligned} \tag{3.11}$$

where we have assumed antiferromagnetic ordering to give the scaling for the momentum variable \mathbf{p} , and the scaling of the field \mathbf{n} is chosen such that $\mathbf{n}^2 = 1$ in the limits $a \rightarrow 0, S \rightarrow \infty$. This follows from

$$S^2(\mathbf{n}_{2j})^2 + a^2(\mathbf{p}_{2j})^2 = S^2 . \tag{3.12}$$

A careful expansion up to a^2 of Hamiltonian (3.1), and the use of (3.12), give within a constant

$$H = H_0 + H_1 , \tag{3.13a}$$

$$\begin{aligned} H_0 &= \frac{cJ}{2} \int dx \left\{ g \left[\mathbf{p} - \frac{\theta}{4\pi} \nabla \mathbf{n} \right]^2 \right. \\ &\quad \left. + \frac{1}{g} \left[(\nabla \mathbf{n})^2 - \left(\frac{\omega_0}{c} \right)^2 (n^z)^2 \right] \right\} , \end{aligned} \tag{3.13b}$$

$$H_1 = \frac{cJ}{2} \int dx \left\{ g \left[\gamma \left[p^z - \frac{\theta}{4\pi} \nabla n^z \right]^2 - \left[\frac{\omega_0 g}{8} \right]^2 (p^z)^2 \right] + \frac{1}{g} \gamma (\nabla n^z)^2 \right\}, \quad (3.13c)$$

where

$$\theta = 2\pi S \quad (3.14)$$

is the topological angle.

The transformation (3.11) differs from the previous transformation given by (3.2), (3.3), and (3.8) through its gradient terms such that the term related with the topological angle appears in (3.13b) but not in (3.7b). Similarly, the H_1 's given by (3.7c) and (3.13c) are slightly different but their structure is the same. By using the same scaling argument as before, we can show that all the terms in H_1 given by (3.13c) are of order g^2 compared with the corresponding terms in H_0 of (3.13b). In leading order in the coupling constant we thus have $H = H_0$ as before. This is the result given by Affleck¹⁴ provided the sign misprint in the definition of ω_0 is corrected for.

The role of the topological angle is to distinguish between the massive and massless versions of H_0 . The model is believed to have a gapless spectrum when θ is an odd multiple of π , i.e., the spin is half-integer, otherwise there is always a finite gap.

In order to compare the predictions obtained in the continuum limit with the results of the lattice model, we will consider now more general Hamiltonians. For arbitrary S the most general isotropic Hamiltonian with nearest-neighbor coupling can be written in the form

$$H = \sum_j h_s(\mathbf{S}_j \cdot \mathbf{S}_{j+1}), \quad (3.15)$$

where $h_s(x)$ is a polynomial of degree S . For special choices of the polynomial the model becomes integrable.^{15,16} Choosing $h_s(x)$ in the form

$$h_s(x) = \sum_{n=1}^{2S} f_n^s \prod_{\substack{m=0 \\ m \neq n}}^{2S} \frac{x - x_m}{x_n - x_m}, \quad (3.16)$$

where

$$x_n = \frac{1}{2}[n(n+1) - 2S(S+1)], \quad (3.17)$$

an antiferromagnetic integrable model is obtained if

$$f_n^s = 4[\psi(n+1) - \psi(1)] = \sum_{m=1}^n \frac{4}{m}, \quad (3.18)$$

where ψ is the logarithmic derivative of the gamma function. The ferromagnetic version of the model has (3.16) with a minus sign; within a constant the same result is given by the choice¹⁷

$$f_n^s = 4[\psi(2S+1) - \psi(n+1)] = \sum_{m=n+1}^{2S} \frac{4}{m}. \quad (3.19)$$

The single-particle excitations of Hamiltonian (3.15) with (3.16)–(3.18), i.e., the antiferromagnetic version, are found¹⁵ to be spin $S = \frac{1}{2}$ excitations with a gapless dispersion law

$$\epsilon(p) = \frac{\pi}{2} \sin p, \quad 0 \leq p \leq \pi. \quad (3.20)$$

Notice that the periodicity of $\epsilon(p)$ is half of the Brillouin zone which is typical of kink-like solutions.

If we apply the transformation (3.11) to the integrable Hamiltonians (3.15), we find easily that in each case the continuum limit is given by H_0 of Eqs. (3.13b) and (3.14) with $\omega_0 = 0$ and a modified sound velocity c . Because the integrable Hamiltonians are known to be gapless for any S , this transformation does not thus give the right critical theory for integer spin.

For this reason Affleck and Haldane¹⁸ re-examined the relation between quantum spin chains and continuum field theories. Starting from a generalized Hubbard model with $2S$ orbitals, which in the $U \rightarrow \infty$ limit is equivalent to the Heisenberg model, the mapping is now to the Wess-Zumino-Witten (WZW) version of the nonlinear sigma model. Due to uncontrollable renormalization effects, the exact equivalence between the parameters of the continuum theory and that of the spin model cannot be established. They argue that in general for integer spin models the relevant operators of the WZW model will be generated and a gap develops. The integrable models with special choices of the couplings correspond to multicritical points.

On the other hand, they claim that for half-integer spins a special topological stability of the model with topological coupling $k=1$ will lead to a behavior analogous to that of the $S = \frac{1}{2}$ model. The integrable higher S half-integer models are again multicritical points in the space of couplings. This seems to be borne out by the numerical calculations¹⁹ for $S = \frac{3}{2}$ models. The absence of a gap for half-integer spins is in agreement with the rigorous argument given recently by Affleck and Lieb²⁰ that if a half-integer spin chain is in a phase with a unique ground state it must have a vanishing mass gap.

Much of the continuum limit analysis described above can be carried over to the composite spin model, Eqs. (2.1) with (2.2). The two transformations, given by Eqs. (3.2), (3.3), and (3.8), and by Eq. (3.11), respectively, cannot be easily applied to the present case because of extra variables per lattice site. On the other hand, these extra variables make the $2 \times S$ model, for example, conform exactly with the nonlinear σ model in terms of variables per lattice site. It is thus possible to construct a single-site transformation²¹

$$\mathbf{n}_j = \frac{(-1)^j}{2S} (\boldsymbol{\sigma}_j - \boldsymbol{\tau}_j), \quad (3.21)$$

$$\mathbf{p}_j = \frac{1}{a} (\boldsymbol{\sigma}_j + \boldsymbol{\tau}_j),$$

where $\boldsymbol{\sigma}_j^2 = \boldsymbol{\tau}_j^2 = S(S+1)$, and the new variables satisfy canonical commutation relations (CCR)

$$\begin{aligned}
[p_j^\alpha, p_j^\beta] &= i\epsilon^{\alpha\beta\gamma} p_j^\gamma a^{-1} \delta_{jj'} \\
[p_j^\alpha, n_j^\beta] &= i\epsilon^{\alpha\beta\gamma} n_j^\gamma a^{-1} \delta_{jj'} \\
[n_j^\alpha, n_j^\beta] &= i\frac{a^2}{4S^2} \epsilon^{\alpha\beta\gamma} p_j^\gamma a^{-1} \delta_{jj'} ,
\end{aligned} \tag{3.22}$$

which in the limit $a \rightarrow 0$, $S \rightarrow \infty$ [$a^{-1} \delta_{jj'} \rightarrow \delta(x-x')$] reproduce the CCR of the nonlinear σ model. The new variables also satisfy relations ($S \rightarrow \infty$)

$$\frac{a^2}{4} \mathbf{p}_j^2 + S^2 \mathbf{n}_j^2 = S^2, \quad \mathbf{p}_j \cdot \mathbf{n}_j = 0. \tag{3.23}$$

We can now make this transformation, for example, on Hamiltonian

$$H_\lambda = J \sum_j [\boldsymbol{\sigma}_j \cdot \boldsymbol{\sigma}_{j+1} + \boldsymbol{\tau}_j \cdot \boldsymbol{\tau}_{j+1} + \lambda(\boldsymbol{\sigma}_j \cdot \boldsymbol{\tau}_{j+1} + \boldsymbol{\tau}_j \cdot \boldsymbol{\sigma}_{j+1})] \tag{3.24}$$

which is the $2 \times S$ version of Hamiltonian (2.1) with (2.2) at the isotropic antiferromagnetic point $J_{xy}^{\alpha\alpha} = J_z^{\alpha\alpha} = -J$, $D^{\alpha\beta} = 0$, and with parametrization (2.3): $J^{\alpha\beta} = \lambda J^{\alpha\alpha}$.

By expanding to second order in a and applying relations (3.23) we find that within a constant factor

$$H_\lambda = \frac{cJ}{2} \int dx [g \mathbf{p}^2 + \frac{1}{g} (\nabla \mathbf{n})^2], \tag{3.25}$$

where $g = S^{-1}(1-\lambda)^{-1/2}$ and $c \equiv 2aS(1-\lambda)^{1/2}$. The topological angle θ is found to be identically zero in this case. We thus find that the continuum limit of the $2 \times S$ model which has always an integer spin at the isotropic antiferromagnetic point is given by the nonlinear σ model with zero topological angle, and has therefore a gap in its excitation spectrum.

The point $\lambda=1$ is a special point of the mapping because there $c, g^{-1} \rightarrow 0$ such that cg is constant. At that point the model can be described by a classical two-dimensional (2D) ferromagnet at a finite temperature, which is known to have an exponentially decaying correlation function. This means that the model has a gap also at $\lambda=1$.

If we add to Hamiltonian (3.24) anisotropic terms corresponding to those in Hamiltonian (3.1),

$$\begin{aligned}
H_2 = J \sum_j \{ & \gamma(\sigma_j^z \sigma_{j+1}^z + \tau_j^z \tau_{j+1}^z) + \mu[(\sigma_j^z)^2 + (\tau_j^z)^2] \\
& + \lambda[\gamma(\sigma_j^z \tau_{j+1}^z + \tau_j^z \sigma_{j+1}^z) + 2\mu\sigma_j^z \tau_j^z] \}, \tag{3.26}
\end{aligned}$$

the same transformation, Eq. (3.21), yields in the continuum limit an anisotropic term

$$\begin{aligned}
H_{2c} = \frac{cJ}{2} \int dx \left[-\frac{1}{g}(1-\lambda) \left(\frac{\omega_0}{c} \right)^2 (n^z)^2 \right. \\
\left. + g(1+\lambda) \left[\frac{\gamma+\mu}{2} (p^z)^2 + \frac{\gamma}{g} (\nabla n^z)^2 \right] \right]. \tag{3.27}
\end{aligned}$$

The first term in H_{2c} is the same ω_0 anisotropy which is included in H_0 in (3.7b) and (3.13b). The other two terms correspond to H_1 in (3.7c) and (3.13c). They can

be disregarded by the same argument as before, and Hamiltonian $H_\lambda + H_{2c}$ provides the same continuum limit description for the composite spin model as H_0 provides for the usual anisotropic Heisenberg model with an integer spin.

Since the topological angle does not depend on the anisotropy we would have to conclude that independently of the anisotropy, the coupling between the two spin species will generate a finite gap for all antiferromagnetic couplings. We will return to this later.

An alternative continuum limit version of the composite spin model can be obtained by applying Abelian bosonization of the fermion description of the $S = \frac{1}{2}$ operators. Following Luther and Scalapino² and den Nijs,²³ Timonen and Luther²⁴ have shown that the spin-1 Heisenberg model can be transformed, in the composite spin representation, first into a fermion problem, and then into a boson problem for the charge and spin densities. The $J_z^{\alpha\beta}$ couplings between the spin species give rise to backward and umklapp scattering between the fermions. These couplings are relevant or irrelevant, depending on the related correlation function exponents. The $J_{xy}^{\alpha\beta}$ coupling between the two species gives rise to a new term which has no exact equivalent in the fermion problem; in a way it is related to the exchange of the two kinds of fermions and is always relevant. By extending the previous analysis²⁴ beyond the planar phase of the model, Schulz²⁵ carried through the corresponding analysis for $2S$ coupled spin- $\frac{1}{2}$ systems to predict the topology of the phase diagram.

Based on these considerations we will try now to predict the phase diagram of the composite spin model. Using first the parametrization in Eq. (2.3) the expected phase diagram in the $(\lambda, J_z/J_{xy})$ plane is shown in Fig. 1. At $\lambda=1$ the composite spin model has the same ground state as the $S=1$ model, so we would have a Heisenberg singlet state in an extended range of anisotropies. For small λ the perturbations proportional to λ are relevant both in the charge and spin-density sector if $J_z/J_{xy} < 0$. The boundaries for small λ and for $\lambda=1$ are supposed to be connected by a smooth curve satisfying the duality relationship. If at $\lambda=1$ the boundaries of the singlet phase are at $J_z/J_{xy} \simeq -1.18$ and $J_z/J_{xy} \simeq -0.1$, as it is supposed from the finite size calculations, and not at points

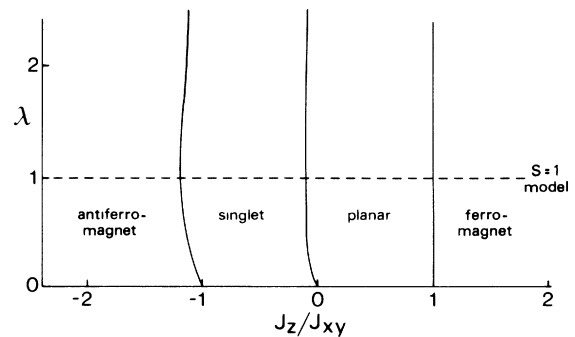


FIG. 1. Expected phase diagram of the $S = 2 \times \frac{1}{2}$ model with parametrization (2.3).

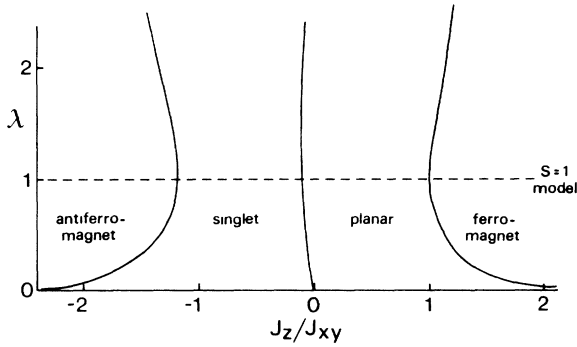


FIG. 2. Expected phase diagram of the $S=2 \times \frac{1}{2}$ model with parametrization (2.8).

determined by symmetry, there is no reason why the boundary should not depend on λ in the composite-spin model.

Using now the parametrization in Eq. (2.8), a different phase diagram is expected, as shown in Fig. 2. At $\lambda=0$ we have two independent XY models. For $J_z < 0$ both the umklapp and the backward scattering terms arising from $J_z^{\alpha\beta}$ become relevant and generate a gap. For small λ , however, the velocity renormalization is small and antiferromagnetism will appear only when $\lambda^{1-q} J_z$ becomes comparable to J_{xy} . Similarly the ferromagnetic boundary is shifted to large anisotropies for small λ . At $\lambda=1$, however, the same boundaries have to be obtained as in Fig. 1, and again the boundaries have to be self-dual.

As we have seen, there are several ways to define a continuum field theory for the spin system and all of them tend to lead to a topologically similar phase diagram, within a variety of approximations. Because of renormalization effects, it is not possible, however, to locate the phase boundaries from the continuum limit, and the subtle features of this limit call for independent, numerical and analytical, evidence resulting from lattice models. The composite spin models in particular provide a unique way to look for crossover effects from a half-integer spin to an integer spin behavior.

IV. COMPOSITE-SPIN $S = \frac{3}{2}$ MODELS

First we consider in more detail the numerical results for composite spin models, which at $\lambda=1$ reduce to the spin- $\frac{3}{2}$ Heisenberg chain. In this case there is now consensus that the isotropic antiferromagnet behaves in the same way as for $S = \frac{1}{2}$, at least as far as the critical behavior is concerned. The spectrum is gapless and the isotropic point separates the planar and antiferromagnetically ordered phases.

There are two ways to construct an $S = \frac{3}{2}$ model: either by having three spin- $\frac{1}{2}$ operators at each site, or one spin- $\frac{1}{2}$ operator and one spin-1 operator. Let us consider first the $3 \times \frac{1}{2}$ model with parametrization (2.3).

As discussed in Sec. II, at $\lambda=0$ the model is decomposed into three independent $S = \frac{1}{2}$ Heisenberg chains. This is a model solvable¹² by a Bethe ansatz, and exact re-

sults are available for the infinite chain problem. Furthermore, there is a recent analysis²⁶ of the scaling behavior of the energy levels for large but finite values of N . As a reference point we can also use results from earlier numerical calculations for this particular case. At $\lambda=1$ the low-lying energy levels of the composite-spin model coincide exactly with those of the $S = \frac{3}{2}$ Heisenberg chain. The extra states introduced by having eight states per site for the three $S = \frac{1}{2}$ spins correspond to replacing the $\frac{3}{2}$ spins at some sites by spin- $\frac{1}{2}$ impurities. The energy of these states is separated by a finite gap of the order J_{xy} from the ground state and are irrelevant when the ground-state degeneracy is studied.

In Fig. 3 we show the energy gap between the ground state and the first excited state as a function of λ for different chain lengths in the isotropic antiferromagnetic point $J_z = -J_{xy} < 0$. At $\lambda=0$ the gap, which is that of the $S = \frac{1}{2}$ Heisenberg chain, scales to zero roughly as $1/N$. A straightforward $1/N$ scaling would, however, predict a small but finite gap at $N = \infty$. This is due to logarithmic corrections in the finite chain calculations. At the isotropic antiferromagnetic point an exact expansion²⁶ gives

$$\Delta E_N(\lambda=0) = \frac{\pi^2}{2N} \left[1 - \frac{1}{2 \ln N} + O \left(\frac{\ln(\ln N)}{(\ln N)^2}, \frac{1}{(\ln N)^2} \right) \right]. \quad (4.1)$$

The true asymptotic behavior is found only for chains with more than 10^3 sites. It was found that if the points for only small values of N are used in fitting the gap, the best fit to the exact Bethe ansatz result is given by

$$\Delta E_N(\lambda=0) = \frac{\pi^2}{2N} \left[1 - \frac{0.435}{\ln N} + \frac{0.234}{(\ln N)^2} \right], \quad (4.2)$$

where we have omitted the small correction to 1 on the

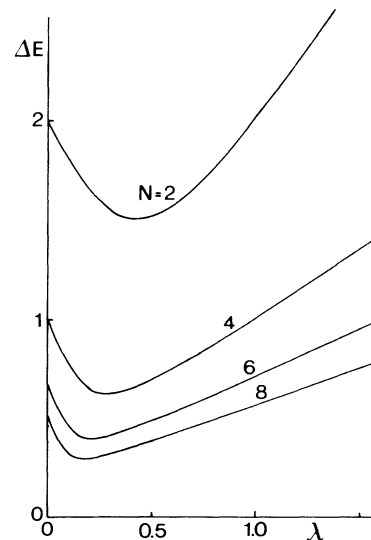


FIG. 3. The primary energy gap of the isotropic $S=3 \times \frac{1}{2}$ model as a function of λ for different chain lengths, using parametrization (2.3).

right-hand side.

For $\lambda > 0$ the gap has a marked minimum whose location approaches the origin roughly as $1/N$ while increasing the chain length; otherwise the gap increases with λ . We conclude that this initial decrease of the gap is a finite size effect, and it can be understood as follows. For finite chains a straightforward perturbational calculation can be done for small λ . As the ground-state wave function for $\lambda=0$ is a product of the singlet wave functions of the independent chains, there is no correction of order λ to the ground-state energy. For the first excited state on the other hand, a degenerate perturbational calculation should be done. Two chains are in their singlet ground state while one chain is in its lowest triplet excited state, yielding altogether a ninefold degeneracy. There will be a correction to the excited state which is linear in λ and lowers the gap. With increasing chain length the singlet-triplet gap decreases as discussed above. The higher-order perturbational corrections become more important and in the limit $N \rightarrow \infty$ the region where the gap decreases will vanish, leading to a λ dependent gap which is nowhere decreasing. We know, however, that at $\lambda=1$, which is the isotropic $S = \frac{3}{2}$ model, the gap should vanish, and therefore the only reasonable conclusion is that the gap vanishes for any λ .

In fact near $\lambda=1$ the gap seems to approach zero roughly as $1/N$. To see better how well the $1/N$ scaling is satisfied, we plot in Fig. 4 the scaled mass-gap ratio. This quantity, which should be unity if the $1/N$ scaling holds exactly, deviates from this value by about 5% when chains with six and eight sites are compared. That the curve is flat over a large region of λ is indicative of a critical behavior for any λ , in agreement with the gapless behavior mentioned above. A naive scaling without taking into account higher order corrections would give a small finite gap in the limit, but if there are corrections like those found at the $\lambda=0$ case, Eqs. (4.1) and (4.2), it would easily explain the difference.

For small λ , however, there are large deviations from unity in the scaled mass-gap ratio. These are due to the marked minima in the gaps themselves in that λ region.

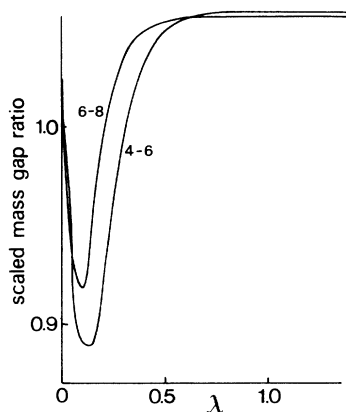


FIG. 4. The scaled mass-gap ratio $(N+2)\Delta E_{N+2}/N\Delta E_N$ for the isotropic $S = 3 \times \frac{1}{2}$ model as function of λ .

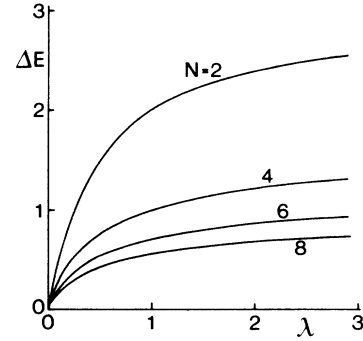


FIG. 5. The primary energy gap of the isotropic $S = 3 \times \frac{1}{2}$ model as a function of λ , using parametrization (2.5b).

As argued before the initial decrease and the minimum in the gap is a finite-size effect, it is due to the fact that in a finite system the singlet ground state and the triplet first excited state are separated by a finite gap and the λ perturbation acts differently on them. In fact, it is seen in Fig. 4 that the dip in the scaled mass gap ratio moves towards $\lambda=0$ and as argued above, it should disappear as $N \rightarrow \infty$.

For comparison we have done the same calculations with the parametrization (2.5b). The primary gap and the scaled mass-gap ratio are shown in Figs. 5 and 6, respectively. For small λ the gap does not scale as $1/N$, in fact the starting slope is roughly N independent but this region is collapsing to the origin as the chain length increases. The scaled mass-gap ratio is flat over the whole λ range, except for very small λ , indicating again a critical behavior for all λ . It should be mentioned, however, that the deviation of the scaled mass-gap ratio from unity is again about 5%.

We have obtained similar results for other parametrizations of the $3 \times \frac{1}{2}$ model. We have also done analogous calculations for the composite spin model which has a spin-1 operator and a spin- $\frac{1}{2}$ operator at each site. The overall behavior of the primary gap is the same as in the

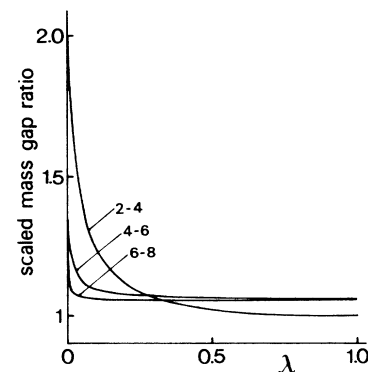


FIG. 6. The scaled mass-gap ratio for the isotropic $S = 3 \times \frac{1}{2}$ model as a function of λ , using parametrization (2.5b).

$3 \times \frac{1}{2}$ model. In fact the interesting levels from parametrization (2.5b) are exactly the same for three $S = \frac{1}{2}$ operators as for an $S = \frac{1}{2}$ and an $S = 1$ operator such that σ_1 is the $S = \frac{1}{2}$ operators, since for the relevant energy levels the two equivalent $S = \frac{1}{2}$ operators in the former case add up to form in effect an $S = 1$ operator.

From this calculation we have to retain two things which will be of importance in the further analysis. The starting slope which is almost independent on N and the sharp dip in the scaled mass-gap ratio are finite-size effects: they do not indicate an exponentially vanishing gap. At the same time a deviation from unity by a few percent of the scaled mass gap ratio at the usual chain lengths is not significant: it does not prove that the gap remains finite in the limit $N \rightarrow \infty$.

V. COMPOSITE-SPIN $S=1$ MODELS

In this section we will consider the spin $S = 2 \times \frac{1}{2}$ model using different parametrizations for the couplings. If the on-site term $D^{\alpha\beta}$ is taken into account, in all the parametrizations mentioned there are three independent coupling constants: λ , J_z/J_{xy} , and D/J_{xy} .

First we will study the stability of the ferromagnetic phase using the parametrization given in (2.3) and (2.9). The boundary of the ferromagnetic phase in the (J_z, D) plane is rather well known for the $S=1$ model, i.e., at $\lambda=1$ in the $2 \times \frac{1}{2}$ model. At $\lambda=0$ this boundary is independent of D , and consists of the line $J_z/J_{xy} = 1$. We show in Fig. 7 the finite-size scaling estimates for this boundary for different values of λ . A remarkable feature of this boundary is that it goes through the point $D=0$, $J_z/J_{xy} = 1$ for all values of λ . In the neighborhood of this point the boundary can be described by

$$D = (J_z - J_{xy}) \frac{1 + \lambda}{\lambda}. \quad (5.1)$$

This curve interpolates smoothly between the two limiting cases, $J_z/J_{xy} = 1$ at $\lambda=0$, and $D = 2(J_z - J_{xy})$ at $\lambda=1$.

For large D/J_{xy} and J_z/J_{xy} the boundary is given by

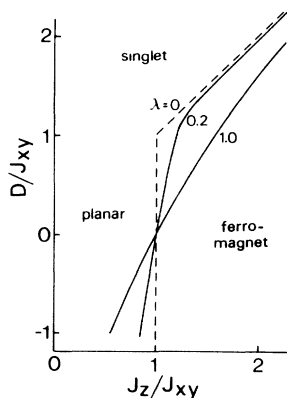


FIG. 7. The phase boundary between the ferromagnetic and planar phases in the (D, J_z) plane for different λ parameters, using parametrization (2.3) and (2.9).

$$D = J_z - \frac{\lambda}{4J_z + \lambda(4D - 2J_z)} \simeq J_z - \frac{\lambda}{2(2 + \lambda)J_z}. \quad (5.2)$$

This expression comes from a perturbational calculation assuming that for large J_z/J_{xy} the σ_1 as well as the σ_2 spins are ordered ferromagnetically, but their mutual orientation depends on the relative importance of H_D and H_{σ_1, σ_2} . Notice that when $\lambda \rightarrow 0$, the phase boundary approaches $D = J_z$, and not $J_z/J_{xy} = 1$. This apparent discrepancy with the D independent phase boundary for the $S = \frac{1}{2}$ chains comes from the fact that the combined ground state of the two decoupled chains is not necessarily ferromagnetic. The two chains can be polarized arbitrarily, relative to each other, and an arbitrary small λ perturbation can lift this degeneracy.

A different situation is expected when the parametrization of Eq. (2.8) is used, and the resulting ferromagnetic phase boundary is shown in Fig. 8 for $q = \frac{1}{2}$. Both here and in the earlier case, the finite-size corrections are very small, the boundaries obtained from chains with six or eight sites differ by less than 1%.

These calculations show that the ferromagnetic phase boundary can be determined with rather high precision from finite chain calculations. The boundaries are λ dependent, except in special cases, where the boundary is determined by symmetries. This again will be important in the further analysis.

We now turn to the most difficult region in the phase diagram, i.e., the neighborhood of the isotropic antiferromagnetic point $J_z/J_{xy} = -1$. If we accept the results of earlier numerical calculations and the predictions for the mappings of spin models to continuum field theories, namely that for the $S=1$ model there is an extended region around the isotropic antiferromagnetic point where the ground state is a singlet, then we expect for the $S = 2 \times \frac{1}{2}$ composite-spin model a phase diagram in the (λ, J_z) plane such as that shown in Figs. 1 or 2, depending on the parametrization.

Figure 9 shows schematically the energy spectrum of the model using Eq. (2.3): (a) for $\lambda=0$, where the spec-

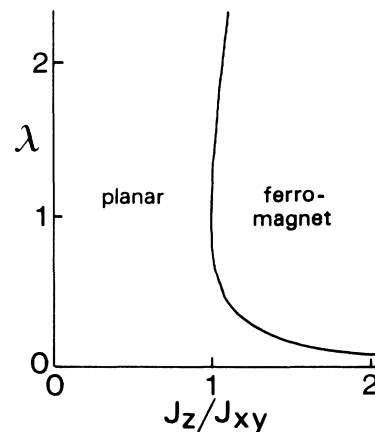


FIG. 8. Phase boundary between the ferromagnetic and planar phases in the $(\lambda, J_z/J_{xy})$ plane, using parametrization (2.8) with $q = \frac{1}{2}$.

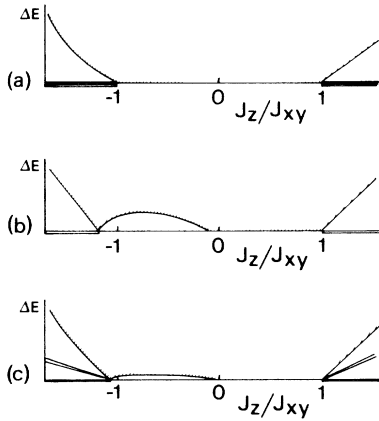


FIG. 9. The energy spectrum relative to the ground state of the $S=2 \times \frac{1}{2}$ model, using the parametrization (2.3). (a) The spectrum in the limit $\lambda=0$, when the model consists of two independent $S=\frac{1}{2}$ chains. The dashed region is a continuum of excitations. (b) The spectrum expected for $\lambda=1$ if a singlet state exists around the isotropic antiferromagnetic point. (c) The spectrum expected for small λ .

trum is just a combination of two identical $S=\frac{1}{2}$ chain spectra, (b) for $\lambda=1$, where the assumed $S=1$ spectrum is shown, and (c) for a small intermediate λ . A weak λ perturbation should give rise only to a slight modification of the spectrum, and if a singlet phase appears near the isotropic point, the gap there should be small. For easy axis anisotropy the boundary between the antiferromagnetic and singlet phases should change continuously from $J_z = -J_{xy}$ at $\lambda=0$ to $J_z = -1.18J_{xy}$ at $\lambda=1$. For easy plane anisotropies the situation is not so clear. Here a small λ perturbation can already remove the ground-state degeneracy as suggested by the continuum limit calculations of Sec. III and thus lead to a singlet state. However, as the boundary between the singlet and planar phases is not determined by symmetry, we would expect it to be λ dependent. Whether the boundary goes to $J_z=0$ as $\lambda \rightarrow 0$, is not clear.

In order to check the picture described above we have calculated the primary gap as a function of λ for different values of J_z/J_{xy} . Using parametrization (2.3) we show in Figs. 10–13 this gap for $J_z/J_{xy} = -0.05, -0.5, -1$, and -1.1 , respectively. At $J_z/J_{xy} = -0.05$ and -0.5 the gap is between the translationally invariant $k=0$ ground state with $S_{\text{tot}}^z=0$ and the first excited state which has $k=0$ and $S_{\text{tot}}^z = \pm 1$, because it contains one spin-flip. At $J_z/J_{xy} = -1.1$ the first excited state is a zone-boundary mode ($k=\pi$) with $S_{\text{tot}}^z=0$, while at $J_z/J_{xy} = -1$ it is threefold degenerate for any λ . The $k=\pi, S_{\text{tot}}^z=0$ mode and the $k=0, S_{\text{tot}}^z = \pm 1$ modes have the same energy.

If the phase diagram shown in Fig. 1 is correct, we should see different behavior as a function of λ depending on whether J_z/J_{xy} is in the range where at $\lambda=1$ the ground state is antiferromagnetic, singlet, or planar.

As is seen in the figures, we find similar behavior for the gap at all values of J_z/J_{xy} . It has a pronounced

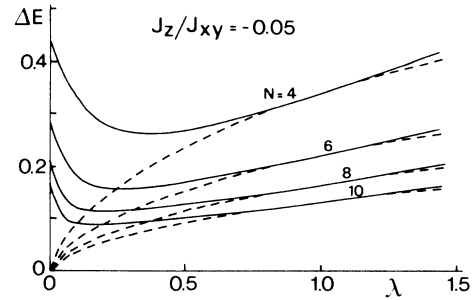


FIG. 10. The primary energy gap of the $S=2 \times \frac{1}{2}$ model as a function of λ for anisotropy $J_z/J_{xy} = -0.05$. N is the number of sites in the chain. The solid lines correspond to parametrization (2.3) while the dashed lines to (2.5a).

minimum for small chain lengths and becomes shallower while increasing the length. The location of the minimum scales towards zero, and beyond the minimum the gap increases monotonically with λ . All curves satisfy the self-duality relation (2.4). At $\lambda=0$ the gap is that of the $S=\frac{1}{2}$ model and its behavior as a function of the chain length is governed by a leading $1/N$ correction, but the logarithmic corrections are important at the available chain lengths. As mentioned in the $3 \times \frac{1}{2}$ case, the minimum in the gap is a typical finite-size effect. Nothing is known about the exact scaling behavior of the gap for finite values of λ . We only notice here, that if at $\lambda=1$ a logarithmic correction is assumed to the simple $1/N$ behavior with unknown coefficients, a fit to the calculated points would still predict a finite gap at $J_z/J_{xy} = -1$. This is valid for longer $S=1$ chains, too, and this is the numerical evidence for the finite gap. Since we have the gap as a function of λ , we can analyze how the $S=\frac{1}{2}$ behavior at $\lambda=0$ goes over into the $S=1$ behavior at $\lambda=1$.

Provided that the continuity assumption holds, in the range $-1.18 \leq J_z/J_{xy} < -1$ there should exist a critical λ_{c_1} below which the gap scales to zero exponentially, giving rise to an antiferromagnetic state. From duality it follows that for $\lambda > \lambda_{c_2} = 1/\lambda_{c_1}$ the system should again have an antiferromagnetic ground state. The singlet

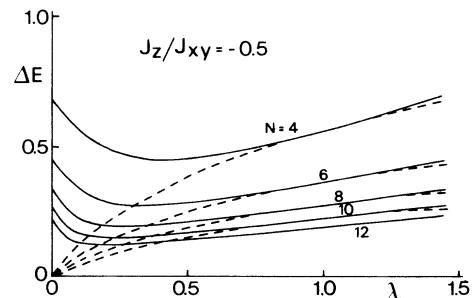


FIG. 11. The same as Fig. 10, for anisotropy $J_z/J_{xy} = -0.5$.

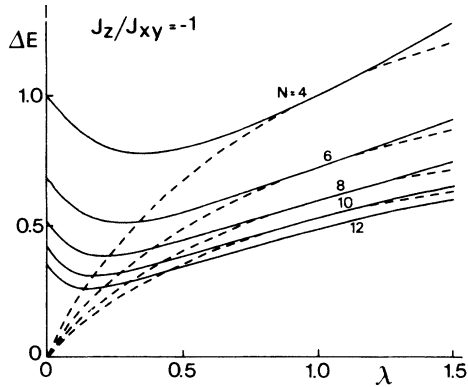


FIG. 12. The same as Fig. 10, for the isotropic antiferromagnetic case.

phase can exist between λ_{c_1} and $1/\lambda_{c_1}$ only. The corresponding λ dependence of the gap is shown schematically in Fig. 14(a).

For small negative J_z ($-0.1 < J_z/J_{xy} < 0$) the situation is different. Here the singlet state should exist for $\lambda < \lambda_{c_1}$ and $\lambda > \lambda_{c_2} = 1/\lambda_{c_1}$, while between λ_{c_1} and $1/\lambda_{c_1}$ the spectrum should be gapless. The λ dependence of the gap in this case is shown in Fig. 14(c). This picture is based on the assumption that the continuum limit gives the phase boundary at $\lambda \rightarrow 0$ correctly. If due to uncontrollable renormalization effects the coupling terms between the two spin species become relevant beyond a finite value of J_z only, there could be a range of anisotropies where the gapless phase exists below λ_{c_1} and above $1/\lambda_{c_1}$, while between these values the gap is finite. Otherwise in the range $-1 < J_z/J_{xy} < -0.1$ the gap should be finite for any finite λ as shown in Fig. 14(b). In Fig. 14 we also show schematically the expected λ dependence of the gap for finite systems. Apart from the initial decrease of the gap, there should be, for long enough chains, a second minimum in cases (a) and (c) either near $\lambda_{c_2} = 1/\lambda_{c_1}$ or near $\lambda = 1$. It should be noticed that duality does not imply that a curve which has a minimum for small λ will necessarily have a second minimum for large

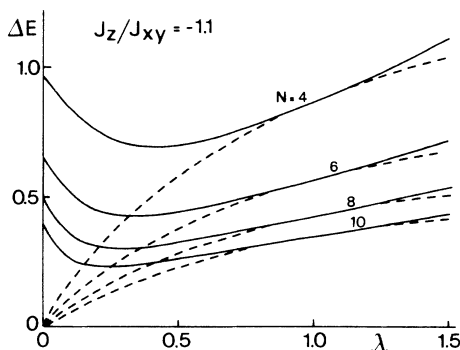


FIG. 13. The same as Fig. 10, for anisotropy $J_x/J_{xy} = -1.1$.

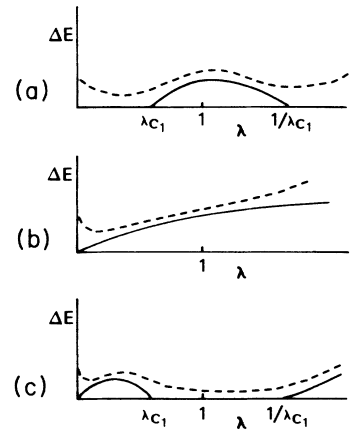


FIG. 14. The expected λ dependence of the gap for various scenarios. (a) The ground state is antiferromagnetic (or planar) for $\lambda < 1/\lambda_{c_1}$, and $\lambda > 1/\lambda_{c_1}$, the singlet state appears in between. (b) The ground state is a singlet for any $\lambda \neq 0$. (c) The ground state is planar or antiferromagnetic between λ_{c_1} and $1/\lambda_{c_1}$, otherwise it is a singlet. The solid lines show the gap for infinite chains, the dashed lines indicate the expected gap for long finite chains.

λ . In fact for the available chain lengths we have never found for any anisotropy a situation where the gap would have a minimum for large λ . The curves are always monotonically increasing with λ beyond the first minimum. The scaling of the first minimum to $\lambda = 0$ and the lack of the secondary minimum indicate that unless there is a crossover at still longer chain lengths, the gap in the infinite chain cannot be a non-monotonic function of λ .

As another check of the size dependence of the gap we plot in Figs. 15–18 the scaled mass-gap ratios for the

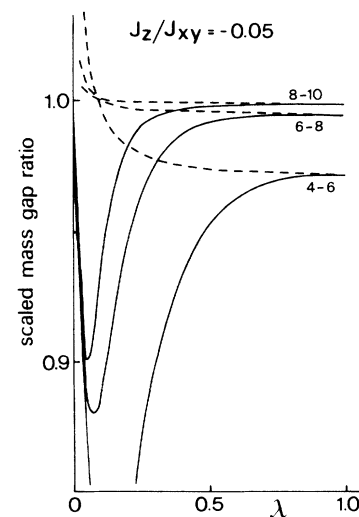


FIG. 15. The scaled mass-gap ratio of the $S = 2 \times \frac{1}{2}$ model as a function of λ for anisotropy $J_z/J_{xy} = -0.05$. The solid lines correspond to parametrization (2.3) while the dashed lines to (2.5a).

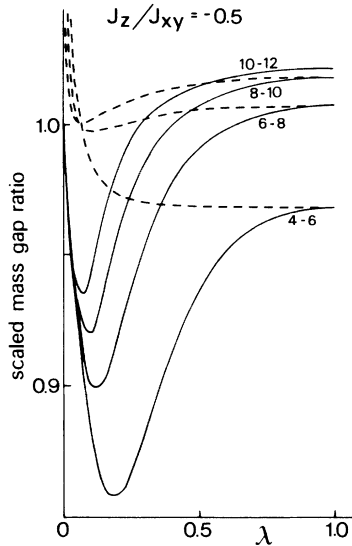


FIG. 16. The same as Fig. 15, for anisotropy $J_z/J_{xy} = -0.5$.

same values of J_z/J_{xy} as used before, i.e., for -0.05 , -0.5 , -1 , and -1.1 respectively. We find a strikingly similar behavior in all these cases: the scaled mass gap ratio is close to unity at $\lambda=0$, as it should be in the $S = \frac{1}{2}$ model, has then the deep minimum, which is a finite-size effect, followed by a broad maximum at $\lambda=1$ very much like in the $3 \times \frac{1}{2}$ case. The scaled mass gap ratio is larger than unity near $\lambda=1$, except for $J_z/J_{xy} = -0.05$. If we assume that at this anisotropy the $S=1$ Heisenberg model has a planar ground state, and that the gap must be a monotonic function of λ , we have to conclude that the gap is zero for any λ . In general, whenever the gap is

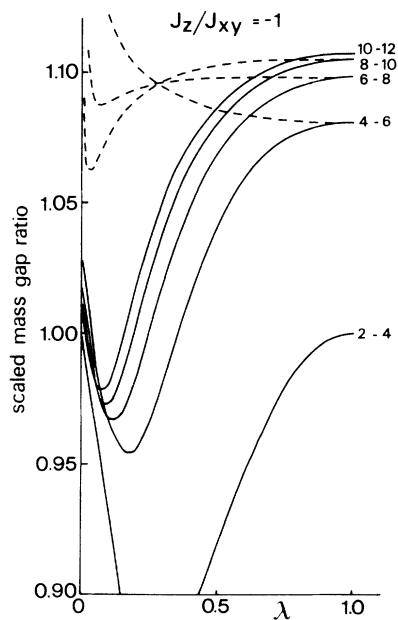


FIG. 17. The same as Fig. 15, for the isotropic antiferromagnetic case.

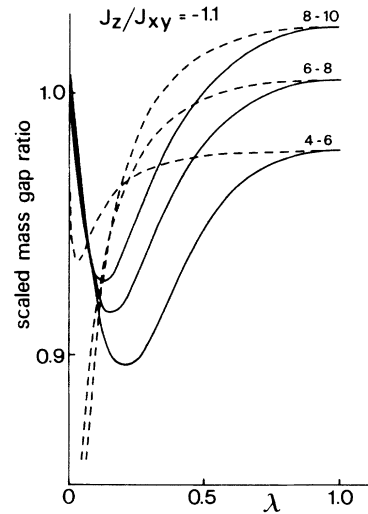


FIG. 18. The same as Fig. 15, for anisotropy $J_z/J_{xy} = -1.1$.

zero at $\lambda=1$, it vanishes for any λ . On the other hand, whenever the gap is finite at $\lambda=1$, the finite chain calculation indicates a finite gap for any finite λ . This would mean a λ -independent boundary between the planar and singlet phases.

A very similar situation occurs in the range $-1.18 \leq J_z/J_{xy} \leq -1$. Here again the finite-size calculations seem to indicate that if the gap is finite at $\lambda=1$, it is finite everywhere, yielding a λ -independent boundary between the singlet and the antiferromagnetic phase. As mentioned before a λ -independent boundary is understandable only if this boundary is determined by symmetry, otherwise there should be a dependence on λ . The continuum limit results are not in agreement with our finite-size calculations, unless the behavior of the gap changes drastically at much longer chain lengths.

We argued that in the limit $N \rightarrow \infty$ the gap is a monotonic function of λ , while for finite N there is always a minimum at a small λ . Other parametrizations can be used to support this conclusion. We show in Figs. 10–13 and 15–18 the gaps and the scaled mass gap ratios for the same anisotropies as before, but calculated with the parametrization (2.5a). These gaps have the following features. At $\lambda=0$ they vanish, since in this case the σ_2 spins are free and can be flipped without cost of energy. At $\lambda=1$ the gaps are identical with those of the $S=1$ Heisenberg model. $\Delta E(\lambda)$ satisfies the duality relationship and is a monotonic function of λ , except for a slight decrease for very large values of λ . However, as the chain length increases, this slight decrease of the gap gets smaller and the positions of the maximum scale towards infinite λ . So, for infinite chains these gaps appear to be monotonic functions of λ . Moreover, comparing with the gaps obtained for the parametrization (2.3) (dashed and solid lines in the figures), we see that a gap for parametrization (2.3) is never smaller than the corresponding gap for parametrization (2.5a), and that they coincide at $\lambda=1$. Combining these results with the general tendencies of the curves, we would again conclude that if at

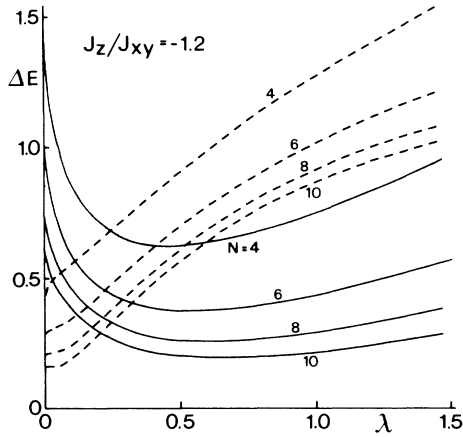


FIG. 19. λ dependence of the gap in the $S = 2 \times \frac{1}{2}$ model using parametrization (2.8) for $J_z/J_{xy} = -1.2$. The solid lines correspond to the gap between the ground state and the first excited state in the sector $S_{\text{tot}}^z = 0, k = \pi$, while the dashed lines correspond to the gap between the ground state and the first excited state in the sector $S_{\text{tot}}^z = \pm 1, k = 0$.

$\lambda = 1$ the gap is finite, it is finite for any $\lambda \neq 0$, while if at $\lambda = 1$ the gap vanishes, it vanishes for all λ .

All parametrizations we have used thus far have conserved the J_z/J_{xy} anisotropy of the model. To test whether this has been essential for the kind of behavior we have found, we shall next use parametrization (2.8) which at $\lambda = 0$ reduces the problem to the $S = \frac{1}{2} XY$ model, and the expected phase diagram which follows from the unrenormalized boson model is shown in Fig. 2. For this model we have calculated the ground state and two relevant excited states which are the lowest state in the $S_{\text{tot}}^z = \pm 1, k = 0$ sector that will indicate a planar phase and the lowest state in the $S_{\text{tot}}^z = 0, k = \pi$ sector that will indicate an antiferromagnetic phase. In Figs. 19–21 we show the result of the finite chain calculations. At the

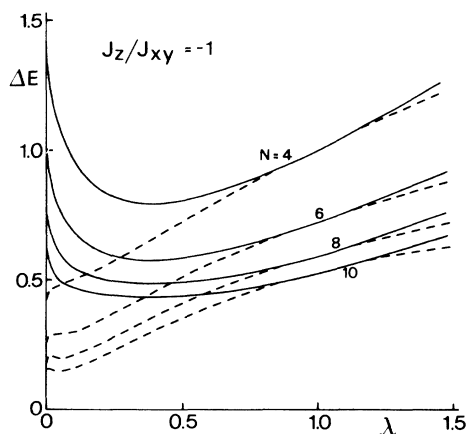


FIG. 20. The same as Fig. 19, for $J_z/J_{xy} = -1$.

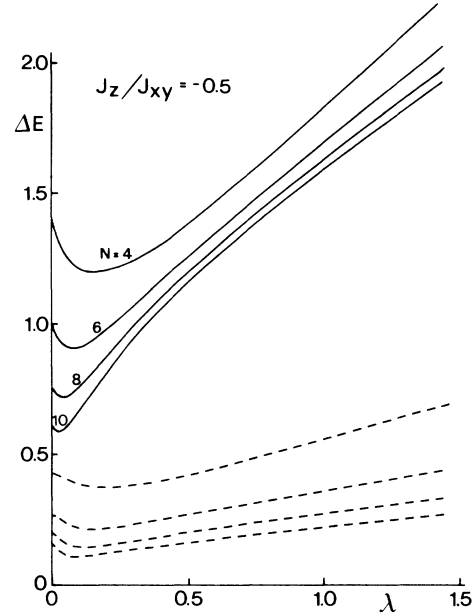


FIG. 21. The same as Fig. 19, for $J_z/J_{xy} = -0.5$.

isotropic antiferromagnetic point and at $J_z/J_{xy} = -0.5$ both gaps seem to remain finite as $N \rightarrow \infty$ for all $\lambda > 0$, in agreement with the continuum limit prediction. At $J_z/J_{xy} = -1.2$ we find, however, a different behavior. Whereas the boson model predicts a singlet state for small enough λ , and a transformation to an antiferromagnetic state with λ increasing, we find that the gap in the $S_{\text{tot}}^z = 0, k = \pi$ sector vanishes for any λ as $N \rightarrow \infty$. The level crossing between the $S_{\text{tot}}^z = 0, k = \pi$ and $S_{\text{tot}}^z = \pm 1, k = 0$ levels seems to scale to a small but finite value of λ , which would indicate that for small λ the gap in the $S_{\text{tot}}^z = \pm 1, k = 0$ sector vanishes also. While this could be a finite-size effect, the vanishing of the other gap does not seem to be questionable. For anisotropies $J_z/J_{xy} < -1.18$ the singlet phase does not appear for any λ . Either the antiferromagnetic phase is realized for all $\lambda > 0$, or a planar ground state for small λ becomes an antiferromagnetic state at a finite λ_c .

The general features of the λ dependence of the gaps are such, that the conclusion is again that if the gap vanishes at $\lambda = 1$ it vanishes for any λ and if it is finite at $\lambda = 1$ it is finite for all $\lambda > 0$, i.e., the phase boundaries seem to be, at least roughly, independent of λ . We would like to point out, however, that our numerical results cannot exclude the possibility that there is no singlet phase at all, and that all the existing evidence for it should be judged with an unbiased mind.

VI. DISCUSSION AND CONCLUSIONS

As discussed in Sec. III, there are a number of possibilities to map lattice-spin models onto continuum field theories. In a sense the most rigorous of these mappings uses non-Abelian bosonization and relates the spin models to Wess-Zumino-Witten-type field theories. These mappings tend to generate a number of relevant opera-

tors, but analytical and numerical results on half-integer spin models on a lattice indicate strongly that there is a kind of “topological stability” of the WZW model with topological coupling $k=1$ and the generic nonintegrable half-integer spin models belong to this universality class. Their spectrum is therefore gapless for $-1 \leq J_z/J_{xy} \leq 1$.

Our numerical results for the composite-spin model which interpolates smoothly between the spin- $\frac{1}{2}$ and spin- $\frac{3}{2}$ cases is in agreement with such a behavior. An exact Bethe ansatz calculation for finite spin- $\frac{1}{2}$ chains gives logarithmic corrections to the N^{-1} scaling of the gap. If the spin- $\frac{3}{2}$ model is described by the same critical theory we would expect it to display similar scaling behavior. If we fit N^{-1} scaling with logarithmic corrections to our spin- $\frac{3}{2}$ data, we indeed find a vanishing gap, while a N^{-1} scaling would give a small but finite gap.

For small λ finite size corrections are more important, the scaled mass gap ratio deviates from unity appreciably, but the range, where this happens shrinks to zero as the chain length increases. At the same time we find further away from this region that with the available chain lengths a deviation from unity by a few percent in the scaled mass-gap ratio is still compatible with a gap that scales roughly as $1/N$.

In the integer spin case all the various mappings lead to a massive singlet phase for antiferromagnetic exchange couplings of the spin models, and there seems to be no “topological conspiracy” to prevent this from happening. For the spin-1 model at the isotropic antiferromagnetic point the numerically calculated scaled mass-gap ratio differs from unity by more than a few percent (it is about 10% at the lengths $N \sim 8, 10, 12$), and even if logarithmic or higher order corrections to the N^{-1} scaling are taken into account, the numerical results indicate a finite gap for infinite chains.

The composite-spin models that interpolate between half-integer and integer spin models provide a unique way to study how exactly the gap opens in the integer spin case, information which is needed to complement continuum limit results which thus far are plagued by uncontrollable renormalization effects. To this end we considered the phase diagram in the $(\lambda, J_z/J_{xy})$ plane of the $2 \times \frac{1}{2}$ model, whose unrenormalized version from the bosonized model was given in Figs. 1 and 2 for parametrization (2.3) and (2.8), respectively. Drawing on the discussion in Sec. V, we show in Fig. 14 the corresponding expected behavior of the gap as a function of λ for different values of the anisotropy J_z/J_{xy} .

In fact we never find in our numerical calculations a gap that as a function of λ would display the expected behavior as shown in Figs. 14(a) and 14(c). From the general features of the λ dependence we find for the gap, we can infer that whenever the gap vanishes at $\lambda=1$ it vanishes for all $\lambda \geq 0$, and a gap such as the one in Fig. 14(c) is never realized in the composite spin model. The possibility which is shown in Fig. 14(a) and should be realized in the anisotropy range $-1.18 < J_z/J_{xy} < -1$ for parametrization (2.3) cannot be categorically excluded, even though there is no indication on the available chain lengths for a nonmonotonic behavior of the gap.

An obvious way to resolve the discrepancy between ex-

pected and numerical results is to claim that the chain lengths we have used are too short for the true asymptotic behavior to show up. The longest chain we could handle numerically had twelve lattice sites which is a typical length in this kind of problem, and gives quite reliable estimates in most cases. Another and we think a more probable way of resolving the discrepancy is to assume that the continuum limit theories gain significant corrections from renormalization effects. This is, in fact, what happens to the planar-ferromagnetic phase boundary: for parametrization (2.3), e.g., it stays at $J_z/J_{xy}=1$ for all λ , even though the bosonization result is $J_z/J_{xy}=\pi/(4+2\lambda)$. Similarly the boundaries between the ferromagnetic, planar and antiferromagnetic phases turn out to be independent of λ in the $S=3 \times \frac{1}{2}$ model for parametrization (2.3), contrary to the prediction of the unrenormalized boson model. This can easily be understood if we accept that in all these cases the phase boundary is determined by symmetry, the phase transition is always at the isotropic point, while in the boson transformation this symmetry is lost.

On the other hand in the cases where symmetry arguments cannot be used, the renormalization effects cannot be easily evaluated. There does not seem to be any reason, however, why the λ dependence should completely be eliminated. One case where finite-size calculation converges well is the location of the ferromagnetic-planar phase boundary for parametrization (2.8). As shown in Fig. 8 there is a marked λ dependence of the boundary in agreement with the expectation. The current³⁻⁷ belief is that in the $2 \times \frac{1}{2}$ model the boundaries of the singlet phase go through $J_z/J_{xy} \simeq -0.1$ and $J_z/J_{xy} \simeq -1.18$ at $\lambda=1$. Since these points are not determined by symmetry, the boundaries of the singlet phase are expected to be λ dependent, as shown in Figs. 1 and 2. The fact that our finite chain calculation indicates a λ -independent boundary for the singlet phase poses a problem. It would be interesting to compare our numerical findings with the renormalization group results for the bosonized model, but the latter calculation is beyond the scope of the present paper.

A word of warning is in place here, however. We have tested numerically the boson predictions for a particular choice of couplings in the $2 \times \frac{1}{2}$ model, where symmetry properties can be used to deduce some general properties of the phase diagram. We find that not even the topology of the phase diagram is given correctly by the bosonized model. It seems that some of the relevant operators in the model are not treated properly in the bosonization, and more analysis is needed if bosonization results are to be extended reliably beyond the planar model as argued²⁴ before. It is evident that in this respect the inclusion²⁵ of Hartree-Fock terms is only a minor correction. A more detailed account of these results will be given elsewhere.

In conclusion, we have shown that the composite spin models allows us to consider the properties of integer and half-integer spin models in the same framework. We have pointed out that the results of the bosonized models exemplifying continuum limit theories which were briefly described for comparison, have to be taken with care because of strong renormalization effects that are not con-

trolled in this particular case. Similarly the results of finite-size scaling on spin chains have to be considered with caution because finite-size corrections on the available chain lengths can make the extrapolation procedure questionable. In particular, the discrepancy between the continuum limit prediction for the interpolation parameter dependence of the singlet phase boundaries and our numerical findings makes it plain that even though, on present evidence, the existence of this phase is plausible, more work is clearly needed to iron out a consistent pic-

ture. Extension of the present analysis to models which interpolate between integrable and nonintegrable models with higher spin lengths is now in progress. We hope that this analysis will clarify some of the very subtle features which seem to make antiferromagnetic models so unexpectedly difficult and interesting to study.

ACKNOWLEDGMENT

We are grateful to Duncan Haldane, Vic Emery, and John Parkinson for useful and enlightening discussions.

*On leave of absence from Central Research Institute for Physics, Budapest, Hungary.

¹J. Sólyom and J. Timonen, *Phys. Rev. B* **34**, 487 (1986).

²F. D. M. Haldane, *Bull. Am. Phys. Soc.* **27**, 181 (1982); *Phys. Rev. Lett.* **50**, 1153 (1983); *Phys. Lett.* **93A**, 464 (1983).

³R. Botet and R. Jullien, *Phys. Rev. B* **27**, 613 (1983); M. Kolb, R. Botet, and R. Jullien, *J. Phys. A* **16**, L673 (1983).

⁴J. C. Bonner and G. Müller, *Phys. Rev. B* **29**, 5216 (1984).

⁵U. Glaus and T. Schneider, *Phys. Rev. B* **30**, 215 (1984).

⁶J. Sólyom and T. A. L. Ziman, *Phys. Rev. B* **30**, 3980 (1984).

⁷J. B. Parkinson, J. C. Bonner, G. Müller, M. P. Nightingale, and H. W. J. Blöte, *J. Appl. Phys.* **57**, 3319 (1985); M. P. Nightingale and H. W. J. Blöte, *Phys. Rev. B* **33**, 659 (1986).

⁸K. Sogo and M. Uchinami, *J. Phys. A* **19**, 493 (1986); M. Takahashi, Technical Report of the Institute for Solid State Phys. (Tokyo), Ser. A, No. 1887, 1988 (unpublished).

⁹H. J. Schulz and T. Ziman, *Phys. Rev. B* **33**, 6545 (1986).

¹⁰A. Moreo, *Phys. Rev. B* **35**, 8562 (1987).

¹¹H. Betsuyaku, *Phys. Rev. B* **36**, 799 (1987).

¹²H. A. Bethe, *Z. Phys.* **71**, 205 (1931); C. N. Yang and C. P.

Yang, *Phys. Rev.* **150**, 321 (1966); **150**, 327 (1966); **151**, 258 (1966).

¹³L. A. Takhtajan and L. D. Faddeev, *Usp. Mat. Nauk.* **34**, 13 (1979).

¹⁴I. Affleck, *Nucl. Phys.* **B257**, 397 (1985); *Phys. Rev. Lett.* **56**, 408 (1986).

¹⁵L. A. Takhtajan, *Phys. Lett.* **87A**, 479 (1982).

¹⁶H. M. Babujian, *Phys. Lett.* **90A**, 479 (1982).

¹⁷F. D. M. Haldane, *J. Phys. C* **15**, L1309 (1982).

¹⁸I. Affleck and F. D. M. Haldane, *Phys. Rev. B* **36**, 5291 (1987).

¹⁹H. J. Schulz and T. Ziman, *Phys. Rev. B* **33**, 6545 (1986).

²⁰I. Affleck and E. Lieb, *Lett. Math. Phys.* **12**, 57 (1986).

²¹L. D. Faddeev and L. A. Takhtajan, Report E-4-83 of the Leningrad Branch of the Mathematical Institute (unpublished).

²²A. Luther and D. J. Scalapino, *Phys. Rev. B* **16**, 1153 (1977).

²³M. den Nijs, *Physica* **111A**, 273 (1982).

²⁴J. Timonen and A. Luther, *J. Phys. C* **18**, 1439 (1985).

²⁵H. J. Schulz, *Phys. Rev. B* **34**, 6372 (1986).

²⁶F. Woynarovich and H.-P. Eckerle, *J. Phys. A* **20**, L97 (1987).